



**Eleventh U.S. National Conference on Earthquake Engineering**  
*Integrating Science, Engineering & Policy*  
June 25-29, 2018  
Los Angeles, California

# COMPUTATIONAL SIMULATION OF DUCTILE FRACTURE IN BUCKLING RESTRAINED BRACES

M.Terashima<sup>1</sup>, G.G. Deierlein<sup>2</sup> and A. Kanvinde<sup>3</sup>

## ABSTRACT

Since their first use in Japan about thirty years ago, Buckling Restrained Braces (BRBs) have been widely implemented in steel-framed buildings throughout the world. To date, most of the development and validation of BRB ductility has relied extensively on testing of full-scale braces under cyclic loading since no fracture evaluation method based on underlying micromechanics is currently available. Therefore, research is currently being undertaken to develop, validate and apply detailed finite element models to computationally simulate ductile fracture initiation and propagation in BRBs. As a part of this research, this paper presents an evaluation methodology of ductile fracture initiation using an Ultra-Low Cyclic Fatigue criterion, referred to as the Stress Weighted Damage Model (SWDM), along with detailed finite element analysis of BRBs.

---

<sup>1</sup> PhD Candidate, John A. Blume Center for Earthquake Engineering, Stanford University, 450 Serra Mall, Stanford, CA 94305 (email: [masaot@stanford.edu](mailto:masaot@stanford.edu)).

<sup>2</sup> Professor, John A. Blume Center for Earthquake Engineering, Stanford University, CA.

<sup>3</sup> Professor, Dept. of Civil and Environmental Engineering, University of California, Davis, CA.



## Computational Simulation of Ductile Fracture in Buckling Restrained Braces

M.Terashima<sup>1</sup>, G.G. Deierlein<sup>2</sup> and A. Kanvinde<sup>3</sup>

### ABSTRACT

Since their first use in Japan about thirty years ago, Buckling Restrained Braces (BRBs) have been widely implemented in steel-framed buildings throughout the world. To date, most of the development and validation of BRB ductility has relied extensively on testing of full-scale braces under cyclic loading since no fracture evaluation method based on underlying micromechanics is currently available. Therefore, research is currently being undertaken to develop, validate and apply detailed finite element models to computationally simulate ductile fracture initiation and propagation in BRBs. As a part of this research, this paper presents an evaluation methodology of ductile fracture initiation using an Ultra-Low Cyclic Fatigue criterion, referred to as the Stress Weighted Damage Model (SWDM), along with detailed finite element analysis of BRBs.

### Introduction

Buckling Restrained Braces (BRBs) are used in lateral force-resistant systems in earthquake prone regions around the world. BRBs consist of a steel core surrounded by restraining members, such as mortar in a casing tube. The detailed geometries of BRBs vary depending on the fabricators and connection types, and their ductility capacity largely depends on these geometries and quality control. Currently, validation of BRB ductility relies on full-scale loading tests under prescribed cyclic loading [1]. Although several studies have proposed ductility evaluation methods [2] [3], they utilized empirically based or statistically based approaches; no study has addressed ductility evaluation based on the underlying fracture mechanism of BRBs.

BRB fracture is usually initiated by ductile fracture due to several large-amplitude cyclic loadings, referred to as Ultra-Low Cyclic Fatigue (ULCF) [4]. The ductile crack usually propagates stably;

---

<sup>1</sup> PhD Candidate, John A. Blume Center for Earthquake Engineering, Stanford University, 450 Serra Mall, Stanford, CA 94305 (email: [masaot@stanford.edu](mailto:masaot@stanford.edu)).

<sup>2</sup> Professor, John A. Blume Center for Earthquake Engineering, Stanford University, CA.

<sup>3</sup> Professor, Dept. of Civil and Environmental Engineering, University of California, Davis, CA

then suddenly changes to a brittle fracture mode, called cleavage. Once cleavage initiates, the crack propagates rapidly, resulting in total fracture of the steel core. This fracture process is not unique to BRBs, but common in many types of structural steel in practice.

This paper describes research to evaluate fracture initiation in BRBs. This study is part of a larger effort to develop and validate computation methods to simulate fracture initiation and propagation in steel structures subjected inelastic cyclic loading due to earthquakes and other hazards.

### Current State of ULCF Criteria and Parameter Calibration

It has been well-accepted that ductile fracture is caused by microvoid nucleation and coalescence. Rice and Tracy theorized that under monotonic tensile loading, the critical equivalent plastic strain ( $\bar{\varepsilon}_p$ ) is correlated exponentially with the degree of hydrostatic confinement, referred to as stress triaxiality ( $T$ ) [5]. Kanvinde et al. [4] modified this ductile fracture criterion to be applicable to cyclic loading (i.e. ULCF) by considering void shrinkage and material deterioration in compression cycle. Smith et al. [6] further improved the ductile fracture criterion to be applicable to wide range of stress triaxiality states and loading conditions. The latest evolution in the local ULCF criterion, the Stress Weighted Damage Model (SWDM), is expressed as follows:

$$D_{SWDM} = e^{\lambda \bar{\varepsilon}_{com}^p} \cdot \int_{\bar{\varepsilon}_p} C (\beta e^{A^+ T} - e^{A^- T}) \cdot e^{\kappa |\xi|} d\bar{\varepsilon}_p \quad (1)$$

where  $D_{SWDM}$  is the damage index for ULCF. The parameters in the equation are calibrated such that fracture is predicted when  $D_{SWDM}$  reaches 1.0.  $A^+$  and  $A^-$  control the triaxiality influence on the growth and shrinkage of voids.  $\beta$  represents the relative rate of void growth and shrinkage,  $\kappa$  the influence of the Lode angle parameter,  $\xi$ , which is the smallest angle between the line of pure shear and the projection of the stress tensor on the deviatoric plane (e.g. axisymmetric loading:  $\xi=1.0$ , plane strain condition:  $\xi=0$ ).  $\lambda$  controls the rate of capacity degradation due to compressive equivalent plastic strain,  $\bar{\varepsilon}_{com}^p$ , while  $C$  represents overall ductility of the material.

These SWDM parameters for A36 steel, which is typically used for the steel core of BRBs, were calibrated using 45 steel notched-bar and plate specimens. The specimens were designed to have various shapes so that the combination of the specimens produces a wide range of stress triaxiality and the Lode angle parameter, ranging from approximately  $0.3 < T < 1.5$  and  $0 < \xi < 1.0$ , respectively. The loading protocols were both monotonic tensile loadings and constant-amplitude cyclic loadings. The cyclic loading protocols consisted of three different amplitude levels to validate the applicability of the SWDM and calibrated parameters under a wide range of amplitude levels. Parameter calibration was carried out using a Maximum Likelihood Estimation (MLE) approach [7], which yields a set of parameter values maximizing the probability of observed results, thereby yielding the following values:  $A^+ = A^- = 1.3$ ,  $\beta = 1.30$ ,  $\kappa = 0.33$ ,  $\lambda = 0.22$  and  $C = 0.1453$ .

### Evaluation of Ductile Fracture Initiation

#### Finite Element Modeling of BRBs

A finite element model of a large-scale BRB was created using ABAQUS [8] to replicate a BRB test designed by Nippon Steel & Sumikin Engineering Co., Ltd, fabricated by Yajima USA, and

tested at the University of British Columbia. The BRB was modeled using twenty-node brick elements with reduced integration (C3D20R in ABAQUS). Uniformly distributed high mode buckling is observed due to the thin layer of unbonding material placed between the steel core and mortar. In this finite element model, the restraining members were not modeled. Instead, inelastic spring constraints were applied at nodes of the steel core where the steel core was constrained by mortar. These inelastic spring constraints have nearly zero stiffness for the first 0.04 inch (i.e. 1mm) elongation, representing the unbonding material thickness. For deformations beyond this gap, the spring stiffness linearly increases to model the constraint effects once the steel core contacts the mortar. An initial imperfection of 0.029 inch (i.e. 0.73mm) of cross-section reduction, corresponding to 1/100 of the entire cross-section, was applied at one-quarter of the length of the steel core to represent fabrication error and to specify the location of necking occurrence. The Armstrong-Frederick model with two nonlinear kinematic backstresses was employed for material plasticity [9]. The material hardening parameters were calibrated using the notched bar and plate tests mentioned in the previous section and the Particle Swarm Optimization (PSO) [6] scheme by minimizing the errors in between the simulated and measured load-deformation response.

The contour plot and the hysteresis are shown in Figures 1 and 2 respectively. Although the FEM result slightly overestimated the force, especially in tensile loading, the FEM generally matched the experimental result. Necking was observed in FEM at the location where section reduction was applied, causing force drop in hysteresis, which was also observed in the experiment. Total failure of the specimen did not occur at the force drop, but in the following cycle.

### **Ductile fracture evaluation**

The ductile fracture evaluations were conducted using the FEM simulation and the SWDM. Three possible locations that ductile fracture may initiate were assumed based on past experiments: 1) edge of shear key, 2) edge of transitional zone and 3) along the yielding zone where necking was observed in FEM (Figure 1). Disassembly of the BRB test specimen analyzed in this study has previously confirmed that the specimen failed at the intermediate section of the steel core (i.e. location 3) as shown in Figure 3. No sign of fracture initiation was observed at other locations.

The local stress/strain histories were simulated using FEM and evaluated using the SWDM equation. Figure 4 shows the ductile fracture evaluation results. The damage index values,  $D_{SWDM}$ , accumulates in tension cycles and reduces in compression cycles, thus having zigzag shapes. The damage index for the location (3) suddenly increased when necking occurred. The damage index at the location (3) exceeded 1.0 slightly after the specimen totally failed in the experiment, while the damage indices were still below 0.4 for other locations. This result shows that fracture initiation is most likely to occur at the location (3), which agrees with the experimental result.

### **Conclusions**

This paper presents a method to evaluate BRB ductile fracture initiation using the SWDM along with the detailed FEM analysis. This fracture evaluation method can reasonably evaluate the experimental result in terms of the location and displacement of fracture initiation. However, local fracture initiation does not necessarily mean total failure of BRBs. As mentioned earlier, BRBs can survive after local ductile fracture initiation. Instead, the total failure of BRBs is usually caused

by cleavage, which is triggered by the ductile crack, but usually occurs after the ductile crack has propagated to a certain length. Further research is currently being undertaken to propose a methodology to simulate the entire fracture process of BRBs.

### Acknowledgments

This research was supported by Nippon Steel & Sumikin Engineering, Co., Ltd. and a grant from the National Science Foundation (CMMI Award #1635043). The authors would also acknowledge University of British Columbia, SIE, Inc and Nippon Steel & Sumikin Engineering USA, Inc for conducting the BRB test and permitting use of the test data.

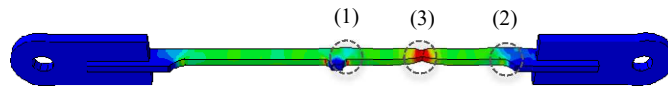


Figure 1 Contour plot showing the equivalent plastic strain at the final step



Figure 3 Disassembly of BRB specimen

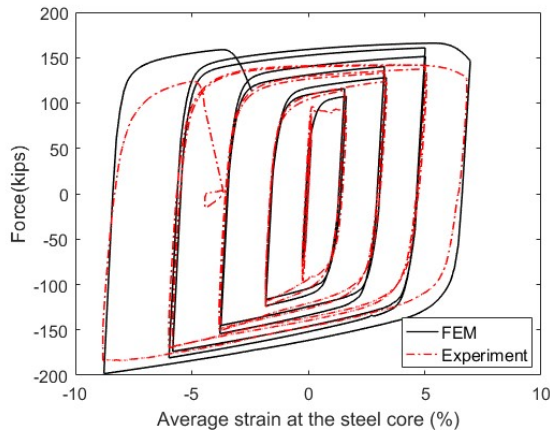


Figure 2 Hysteresis behavior of BRB

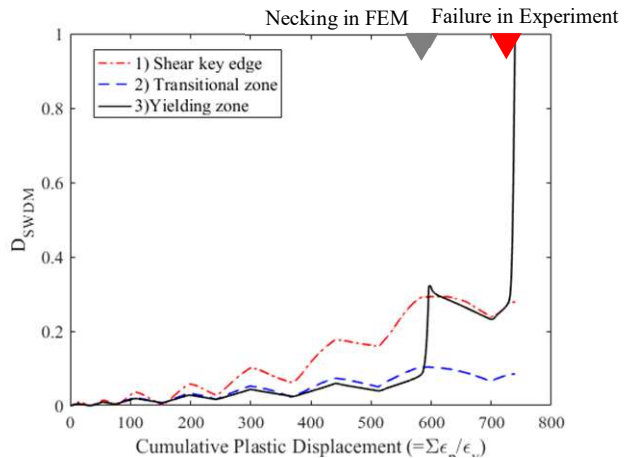


Figure 4. Ductile fracture evaluation results

### References

- 1 AISC-341-10, "Seismic Provisions for Structural Steel Buildings (ANSI/AISC41-10)," *Am. Inst. Steel Constr.*, 2010.
- 2 H. Nakamura *et al.*, "Fatigue Properties of Practical-Scale Unbanded Braces," *Nippon Steel Corp. Tech. Rep.*, pp. 49–55, 1999.
- 3 T. Takeuchi, M. Ida, S. Yamada, and K. Suzuki, "Estimation of Cumulative Deformation Capacity of Buckling Restrained Braces," *J. Struct. Eng.*, vol. 134, no. 5, pp. 822–831, 2008.
- 4 A. Kanvinde and G. G. Deierlein, "Cyclic Void Growth Model to Assess Ductile Fracture Initiation in Structural Steels due to Ultra Low Cycle Fatigue," *J. Eng. Mech.*, vol. 133, no. 6, pp. 701–712, 2007.
- 5 J. R. Rice and D. M. Tracey, "On the ductile enlargement of voids in triaxial stress fields," *J. Mech. Phys. Solids*, vol. 17, no. 3, pp. 201–217, 1969.
- 6 C. M. Smith, A. M. Kanvinde, and G. G. Deierlein, "Stress-Weighted Damage Model for ductile fracture initiation in structural steel under cyclic loading and generalized stress states," Stanford University, 2014.
- 7 A. T. Myers, G. G. Deierlein, and A. Kanvinde, "Testing and Probabilistic Simulation of Ductile Fracture Initiation in Structural Steel Components and Weldments," Stanford University, 2009.
- 8 Dassault Systèmes Simulia, "Abaqus CAE User's Manual," *Abaqus 2017*, p. 1174, 2017.
- 9 P.J. Armstrong, C.O. Frederick, A mathematical representation of the multiaxial Bauschinger effect, CEGB Report, RD/BN731Berkeley Nuclear Laboratories, 1966.